# Supporting information

# Insights into the photocatalytic mechanism of g-$C_3N_4$/$Cs_2BBr_6$ (B = Pt, Sn, Ti) heterojunction photocatalysts by density functional theory calculations

Xinyu Ye[a,b], Yuanmiao Sun[b,*], Anmin Liu[c,*], Shizheng Wen[d], and Tingli Ma[a,*]

[a] Graduate School of Life Science and Systems Engineering, Kyushu Institute of Technology, 2-4 Hibikino, Wakamatsu, Kitakyushu, Fukuoka 808-0196, Japan.

Email: tinglima@life.kyutech.ac.jp

[b] Institute of Technology for Carbon Neutrality, Shenzhen Institute of Advanced Technology, Chinese

Academy of Sciences, Shenzhen 518055, China.

Email: sunym@siat.ac.cn

[c] State Key Laboratory of Fine Chemicals, School of Chemical Engineering, Dalian University of Technology, China.

Email: liuanmin@dlut.edu.cn

[d] School of Physics and Electronic Electrical Engineering, Huaiyin Normal University, Huai'an, 223300, China.

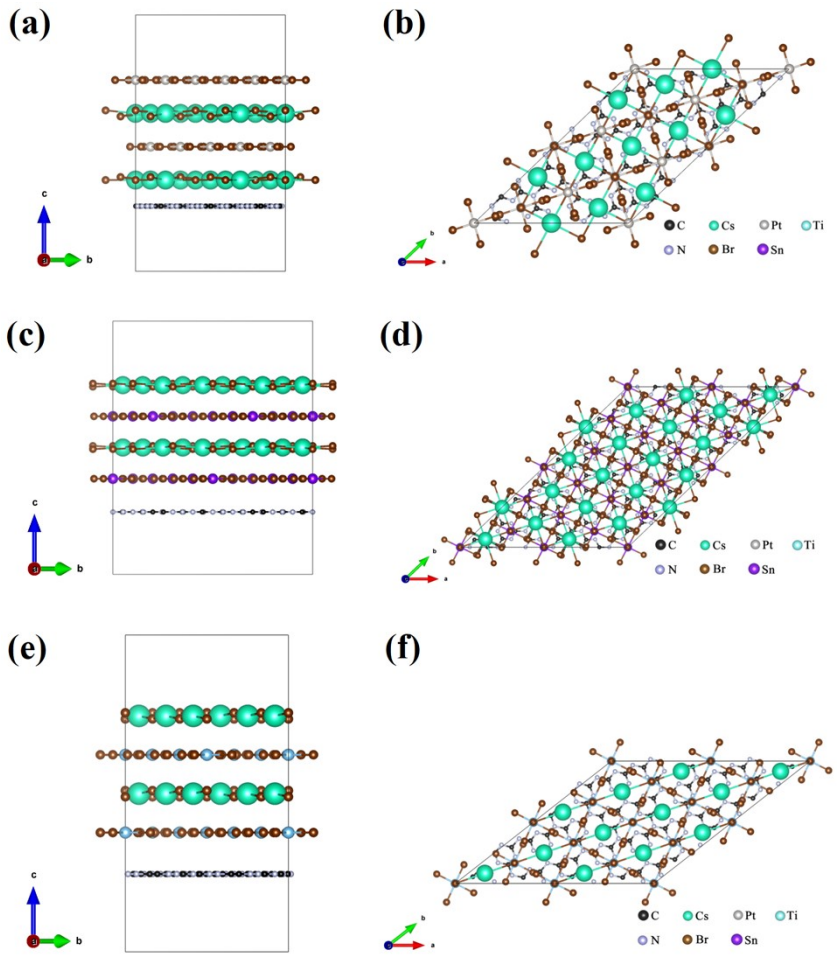


**Fig. S1** Theoretical models for (a, b) g-$C_3N_4$/$Cs_2PtBr_6$, (c, d) g-$C_3N_4$/$Cs_2SnBr_6$, and (e, f) g-$C_3N_4$/$Cs_2TiBr_6$ heterojunctions.

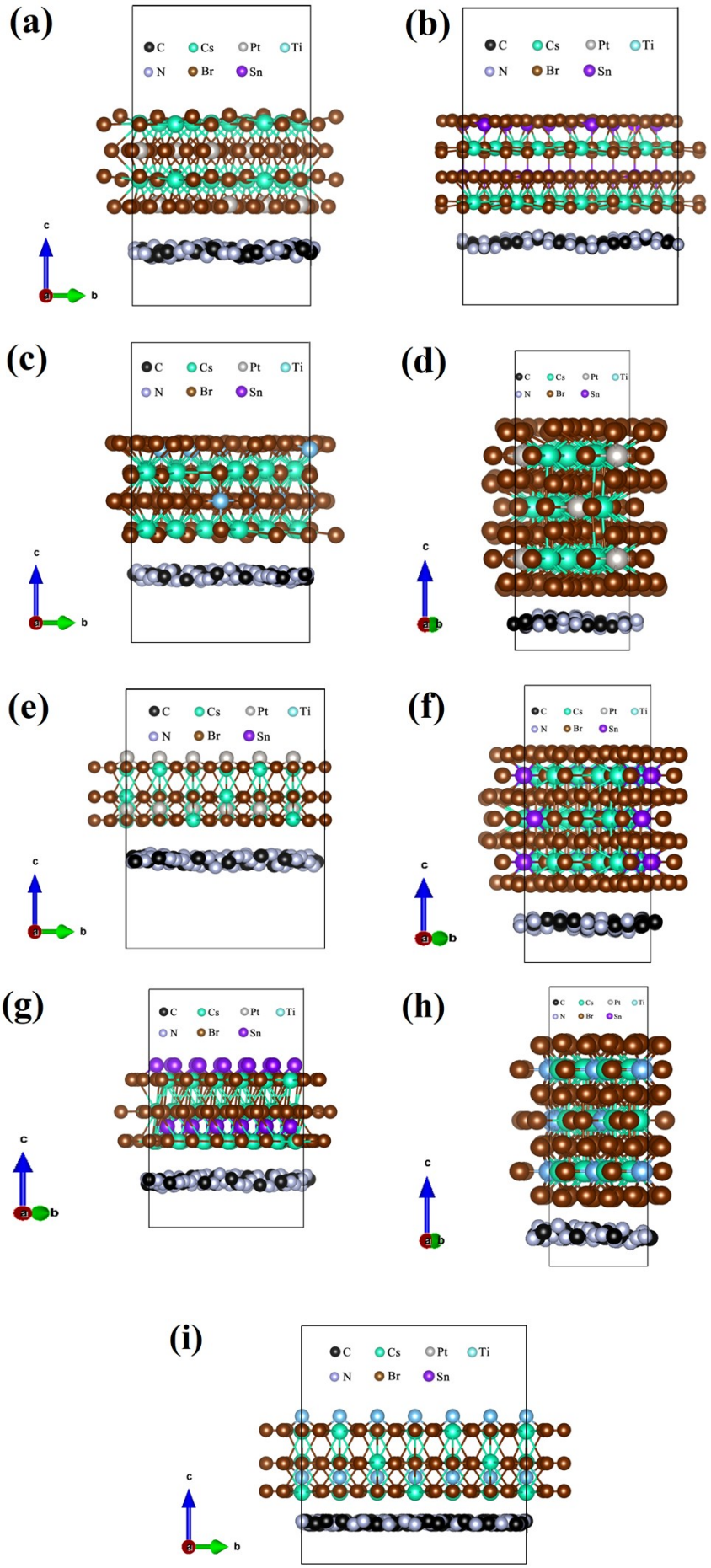
(a)
(b)
(c)
(d)
(e)
(f)
(g)
(h)
(i)
C Cs Pt Ti
N Br Sn
c
b

**Fig. S2** Optimized geometric structures of (a) g-$C_3N_4$/$Cs_2PtBr_6$(001) heterostructure with Pt-terminated surface, (b) g-$C_3N_4$/$Cs_2SnBr_6$(001) heterostructure with Cs-terminated surface, (c) g-$C_3N_4$/$Cs_2TiBr_6$(001) heterostructure with Cs-terminated surface, (d) g-$C_3N_4$/$Cs_2PtBr_6$(110) heterostructure, (e) g-$C_3N_4$/$Cs_2PtBr_6$(111) heterostructure, (f) g-$C_3N_4$/$Cs_2SnBr_6$(110) heterostructure, (g) g-$C_3N_4$/$Cs_2SnBr_6$(111) heterostructure, (h) g-$C_3N_4$/$Cs_2TiBr_6$(110) heterostructure and (i) g-$C_3N_4$/$Cs_2TiBr_6$(111) heterostructure.

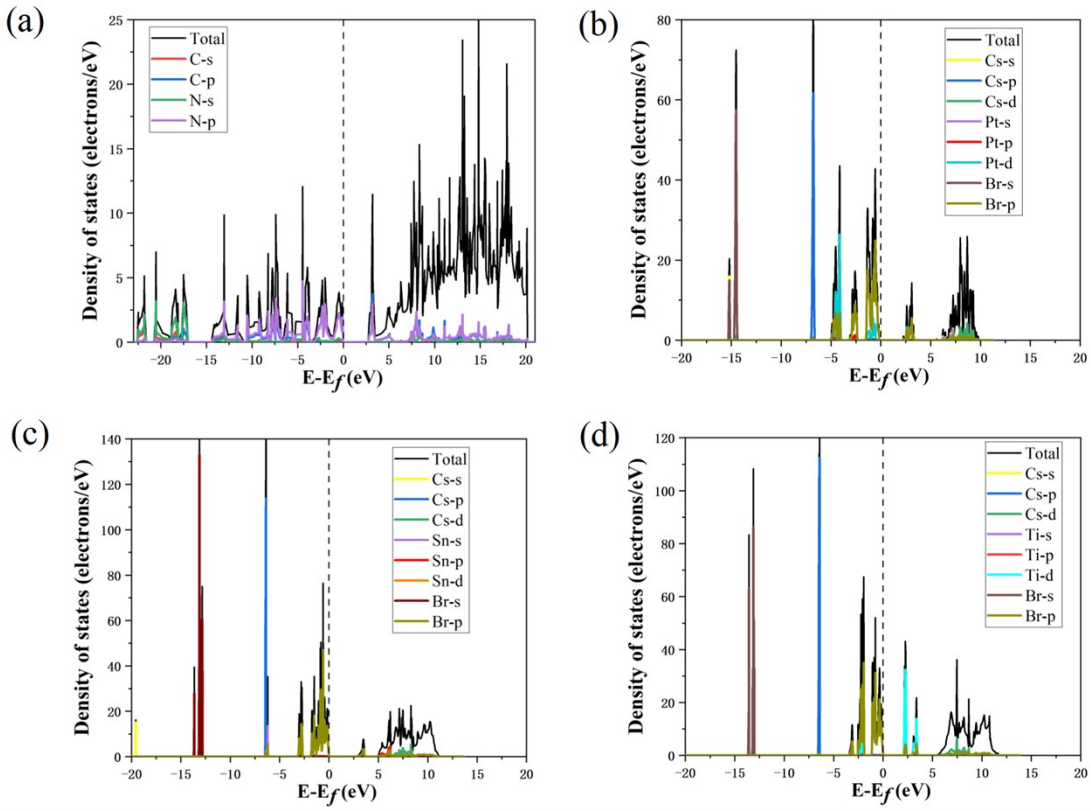


**Fig. S3** Calculated TDOS and PDOS of (a) monolayer g-$C_3N_4$, (b) $Cs_2PtBr_6$(001) slab, (c) $Cs_2SnBr_6$(001) slab, (d) $Cs_2TiBr_6$(001) slab over a wider energy range (-20 eV to 20 eV). The black vertical line is Fermi level.

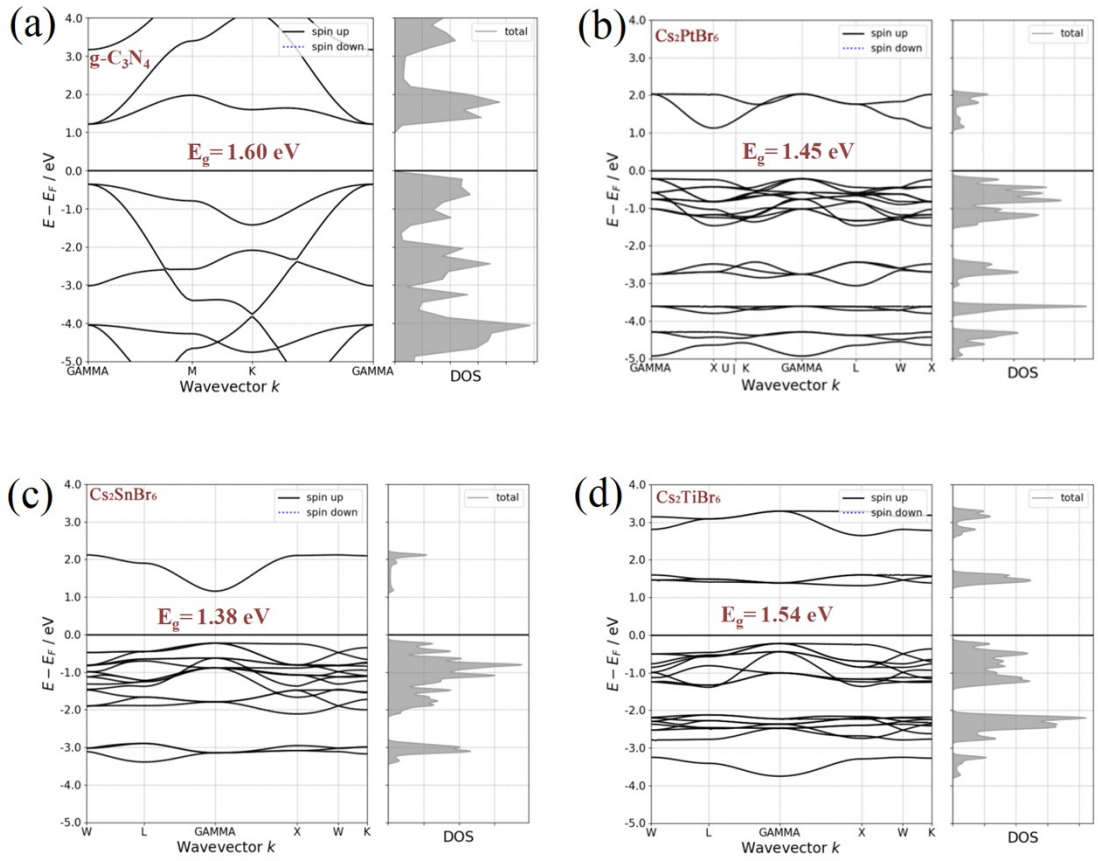


**Fig. S4** Band structures and density of states of the (a) g-$C_3N_4$, (b) $Cs_2PtBr_6$, (c) $Cs_2SnBr_6$, (d) $Cs_2TiBr_6$ calculated by PBE functional.

**Table. S1** Binding energies (eV) of g-$C_3N4$/$Cs_2PtBr_6$ heterojunctions with varying $Cs_2PtBr_6$ components.

| Species | (001) plane | (110) plane | (111) plane | Pt-terminated |
|---|---|---|---|---|
| Binding energy (eV) | -4.25 | -3.86 | -3.08 | -3.82 |
| Mismatch energy (eV) | 4.15 | 4.22 | 4. 65 | 4.47 |

**Table. S2** Binding energies (eV) of g-$C_3N4$/$Cs_2SnBr_6$ heterojunctions with varying $Cs_2SnBr_6$ components.

| Species | (001) plane | (110) plane | (111) plane | Cs-terminated |
|---|---|---|---|---|
| Binding energy (eV) | -1.65 | -1.01 | -1.50 | -1.60 |
| Mismatch energy (eV) | 10.26 | 11.28 | 10.36 | 10.31 |

**Table. S3** Binding energies (eV) of g-$C_3N4$/$Cs_2TiBr_6$ heterojunctions with varying $Cs_2TiBr_6$ components.

| Species | (001) plane | (110) plane | (111) plane | Cs-terminated |
|---|---|---|---|---|
| Binding energy (eV) | -2.88 | -2.27 | -2.00 | -2.80 |
| Mismatch energy (eV) | 6.26 | 6.66 | 7.05 | 6.35 |

**Table. S4** Average Bader atomic charge (e), the minimum distance (Min dist. (Å)), and valency in isolated $Cs_2PtBr_6$ and g-$C_3N_4$.

| Atom | C | N | Cs | Pt | Br |
|---|---|---|---|---|---|
| Average Bader charge (e) | 0.64 | 7.47 | 8.04 | 9.52 | 7.55 |
| Valency | 3.36 | -2.47 | 0.96 | 0.48 | -0.55 |

**Table. S5** Average Bader atomic charge (e), the minimum distance (Min dist. (Å)), and valency in isolated $Cs_2SnBr_6$ and g-$C_3N_4$.

| Atom | C | N | Cs | Sn | Br |
|---|---|---|---|---|---|
| Average Bader charge (e) | 0.88 | 7.20 | 8.01 | 11.92 | 7.90 |
| Valency | 3.12 | -2.20 | 0.99 | 2.08 | -0.90 |

**Table. S6** Average Bader atomic charge (e), the minimum distance (Min dist. (Å)), and valency in isolated $Cs_2TiBr_6$ and g-$C_3N_4$.

| Atom | C | N | Cs | Ti | Br |
|---|---|---|---|---|---|
| Average Bader charge (e) | 0.94 | 7.17 | 8.01 | 7.89 | 7.94 |
| Valency | 3.06 | -2.17 | 0.99 | 2.11 | -0.94 |